AC Resistance of Planar Power Inductors and the Quasidistributed Gap Technique

Jiankun Hu
C. R. Sullivan

From *IEEE Transactions on Power Electronics,* vol. 16, no. 4, pp. 558–567.

AC Resistance of Planar Power Inductors and the Quasidistributed Gap Technique

Jiankun Hu and Charles R. Sullivan, *Member, IEEE*

***Abstract*—Low-ac-resistance planar or foil-wound inductors constructed using a quasidistributed gap comprising multiple small gaps that approximate a distributed gap are analyzed. Finite-element simulations are used systematically to develop a model broadly applicable to the design of such quasidistributed gap inductors. It is shown that a good approximation of a distributed gap is realized if the ratio of gap pitch to spacing between gap and conductor is less than four, or if the gap pitch is comparable to a skin depth or smaller. Large gaps can reduce ac resistance, but for most practical designs gap length has little effect. A closed-form expression, which closely approximates the ac resistance factor for a wide range of designs, is developed. The methods are illustrated with an inductor for a high-ripple-current fast-response voltage regulator module (VRM) for microprocessor power delivery.**

***Index Terms*—Air gaps, distributed gaps, eddy currents, fringing effects, inductors, magnetic devices, power conversion, proximity effect, quasidistributed gaps, skin effect, voltage regulator modules.**

I. Introduction

CONDUCTOR losses in high-frequency magnetic components are strongly influenced by the magnetic field distribution in the winding area. For transformers, it is relatively straightforward to understand and to control the field and the resulting losses. However, in inductor designs, the field configuration is influenced by the geometry and position of the gap as well as the conductors. Avoiding excessive losses can be challenging.

Planar configurations are often desirable for inductors because of packaging constraints, because of fabrication technology, or because of thermal considerations. A planar configuration has the potential for particularly high ac conductor losses. Sheets of conductor are prone to high eddy currents if there is a vertical field component perpendicular to the sheet. Gaps in the magnetic path tend to introduce such a perpendicular field component [1]–[6]. One of the most elegant solutions to this problem is to use a low-permeability material to effect a distributed gap across the top of the planar conductor [2], as shown in Fig. 1. With a distributed gap, field lines are parallel to the surface of the conductor, and they do not affect the lateral distribution of the current, which flows uniformly across the top surface of the conductor, with current density decaying exponentially with depth according to standard skin-effect behavior.

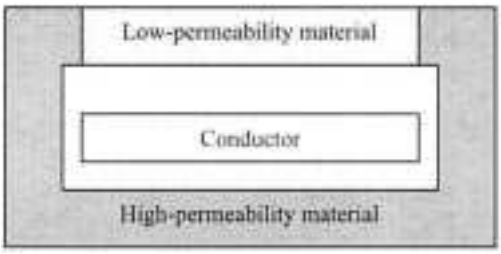

Fig. 1. Distributed-gap inductor: use of a low-permeability material to achieve low ac resistance.

Although powdered iron and other more specialized materials can provide the low permeability needed for a distributed gap [7], typical high-performance power ferrite materials are too high in permeability for direct use in a distributed gap. For this reason, the *quasidistributed gap* has been proposed as an alternative to the true distributed gap for planar inductors and for more conventional wire-wound and foil-wound components [4]–[6], [8]–[14]. This alternative, sometimes called a *discretely distributed gap*, uses multiple small gaps to approximate a lower-permeability material, as shown in Fig. 2.

Although the principle of quasidistributed gaps is well established, adequate design rules have not previously been developed. For example, it is not immediately clear how many small gaps are necessary to approximate a distributed gap. For any given design, it is possible to use finite-element simulations to calculate losses, and use trial and error to find a design that works adequately. But this is not an efficient approach in practical design. It would be preferable to be able to calculate or estimate the requirements for a quasidistributed gap, to guide design without the need for repeated simulations.

An intuitive rule of thumb might be to space the conductor away from the gaps by a distance that is large compared to the gap length, to keep the fringing field from the gap away from the conductor. However, previous work has shown that this can result in losses nearly three times higher than losses with a true distributed gap [9]. Simulations or measurements of other designs show that losses can be much closer to those calculated for a true distributed gap [6], even within a few percent [4]. These discrepancies show that the idea of keeping the spacing large compared to the gap length is not adequate or correct. Analytical calculations for geometries like this are possible [15], but yield highly complex results that are difficult to use in design. In this paper, a parametric study of losses is used to identify what the important relationships actually are. This approach, introduced in [16], has also been used in [17] to analyze other winding

Manuscript received March 8, 2000; revised April 16, 2001. Recommended by Associate Editor K. Ngo.

J. Hu is with the Agere Systems, Allentown, PA 18109 USA (e-mail: huj1@lucent.com).

C. R. Sullivan is with the Thayer School of Engineering, Dartmouth College, Hanover, NH 03755 USA (e-mail: charles.r.sullivan@dartmouth.edu).

Publisher Item Identifier S 0885-8993(01)05957-9.

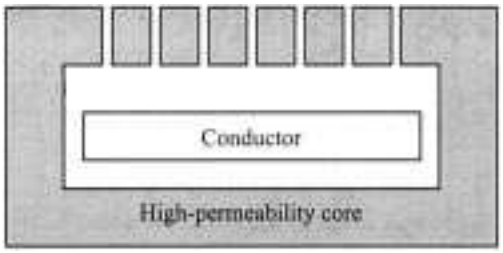

Fig. 2. Quasidistributed gap inductor using multiple small gaps to approximate a distributed gap.

loss problems. The systematic set of numerical simulations is used to establish a set of rules and closed-form approximations that will allow designers to much more easily use a quasidistributed gap to match the performance of a distributed gap. Unlike most results from finite-element simulations, these results are general and apply to a wide range of designs. Thus, they can been applied to designs ranging from 5–10 MHz microfabricated thin-film inductors operating at power levels under 10 W such as those in [4], [5] to 100 kHz ferrite-core designs for tens of kVA such as those in [14]. The results are stated in terms of dimensions normalized to skin depth, such that there is no limit to the size, power level, or frequency at which they are applicable.

The generality of the results also means that they can be used to analyze inductors with any number of gaps, including those with only a single gap. Thus, the results can be used to avoid the need for multiple gaps, by showing what conditions ensure low ac resistance even with a single gap. The use of the method for a case that might not ordinarily be considered a quasidistributed gap will be illustrated with a design example in Section IV.

In a practical design of an inductor, there are many issues that must be considered. In this paper, we thoroughly analyze the issue of approximating a distributed gap with a quasidistributed gap, rather than attempting to survey inductor design more generally. For example, we do not consider core loss (which may be complicated by the effects of dc bias and nonsinusoidal waveforms [18]–[20]) or the design tradeoff between winding and core loss. The cross sections shown in Figs. 1 and 2 are two-dimensional, and, especially for a multiturn winding, there must be some provision for the windings to close, in the third dimension, either with an axially symmetric pot-core-like structure or with an E-core-like structure with an end-turn region. In either case, there would be additional issues that are not considered here with the ac resistance effects in the end turns, or with the effect of the curvature in a pot-core-like structure [21]. Another issue not addressed in this paper is the validity of the finite-element analysis methods used. Finite-element analysis (FEA) for electromagnetics is based on applying well-established numerical methods—now widely used for thermal systems, fluids, semiconductors, and many other types of systems—to the solution of Maxwell's equations. FEA has been successfully used for loss predictions in high-frequency windings for power electronics since at least 1985 [22]. Numerical methods are usually verified by comparison with analytical solutions on problems for which such solutions exist, but power electronics researchers have also checked consistency with experimental measurements with good results, for example in [23]–[27]. The small discrepancies between FEA and experimental results in [23]–[27] are attributed to limited accuracy of experimental measurements or to aspects of the experimental structure that have not been modeled in the FEA, such as the termination impedance or three-dimensional effects discussed above. In no case is there evidence suggesting flaws in the FEA results. Thus, we consider the reliability FEA to be well established, and we have not sought to do our own experimental verification of it.

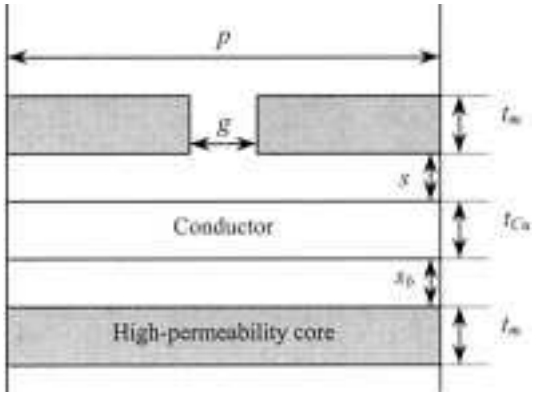

Fig. 3. Section of a quasidistributed gap used for simulation. Dimensions are normalized to one skin depth in the conductor.

A. Problem Definition and Simplification

We wish to reduce the problem to the minimum essential framework, to facilitate computations and conceptual understanding. To do this, we assume an infinitely wide quasidistributed gap inductor. In this infinitely wide strip, with an infinite number of gaps, each gap is equivalent.[1] This means that we can base our simulation on only a single gap, as shown in Fig. 3, with symmetry boundaries on the left and right.

We can describe this structure in terms of six geometric parameters as shown in Fig. 3: gap pitch p, gap length g, the space between the conductor and the gaps s, the thickness of the core $t_{\rm m}$ (assumed equal for top and bottom core sections), the thickness of the conductor $t_{\rm Cu}$, and the spacing between the lower core and the conductor $s_{\rm b}$. We normalize all these dimensions in terms of skin depth in the conductor material, $\delta = 1/\sqrt{\pi \cdot f \cdot \mu_0 \cdot \sigma}$, where

f frequency;
μ_0 permeability of free space;
σ conductivity of the conductor.

We assume the permeability of the magnetic material is infinite.

If the quasidistributed gap is effective at approximating a distributed gap, the choice of conductor thickness is already well understood: since current will mainly flow in the top skin depth, a thickness of one to two skin depths is sufficient to achieve near-minimum ac resistance. Thicker conductors can be used, but they will decrease only dc resistance. Thus, we perform most of our simulations with a conductor two-skin-depths thick. Since the field has decayed to near zero at the bottom of the conductor, the spacing to the back magnetic material, $s_{\rm b}$, is not important. The thickness of the core material is also unimportant

[1]An infinitely wide strip like this is an ill-posed problem, in that the inductance per unit width becomes undefined, but this is not important to the results here.

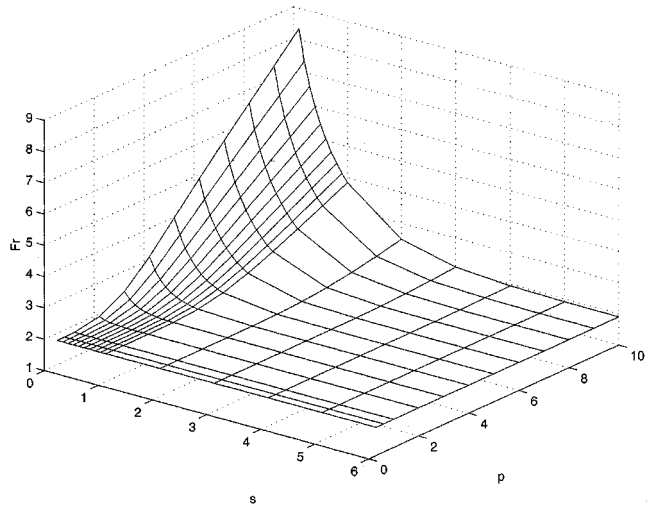

Fig. 4. Simulated ac resistance factor, F_r as a function of gap pitch p, and the conductor–gap spacing s, both normalized to skin depth. The gap length was 0.1 (one tenth of a skin depth) for these simulations; however, the results apply for any small gap ($g < 0.3$; see the text for a more detailed discussion of gap length effects).

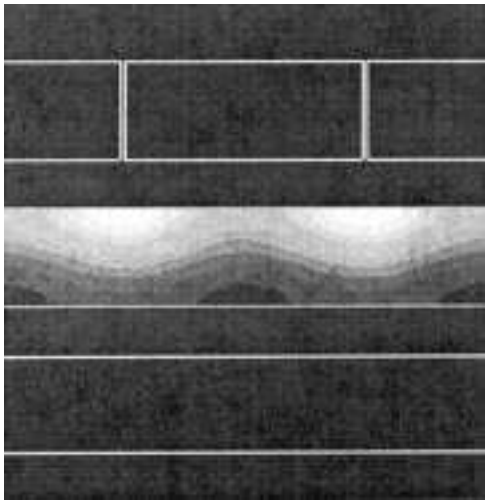

Fig. 5. Current distribution in a cross section of a quasidistributed gap inductor. Lighter shading indicates higher current regions. Dimensions as defined in Fig. 3, normalized to a skin depth, are $p = 5$, $s = 1$, and $g = 0.1$.

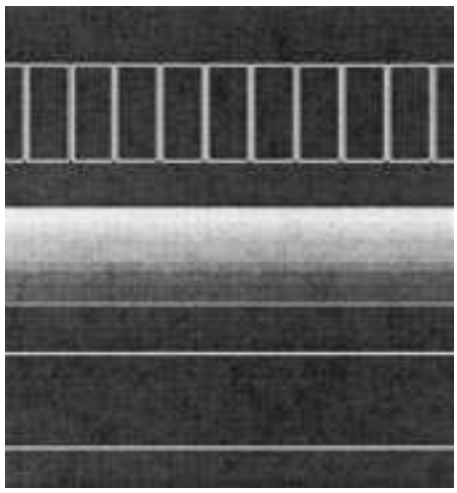

Fig. 6. Current distribution in a cross section of a quasidistributed gap inductor. As in Fig. 5, but with a smaller gap pitch of $p = 1$ skin depth.

for the present purposes, as will be demonstrated in Section II-E. This leaves as parameters only g, s and p as shown in Fig. 3. By using a systematic approach to these variables, and by exploiting the symmetry of the problem to allow finite-element simulation of a section of length equal to only one gap pitch[2], it is possible to generate sufficient simulation data to understand the problem thoroughly.

II. Simulation Results and Analysis

A. Simulation Results

The results of simulations are plotted in Fig. 4, which shows the ac resistance factor, $F_r = R_{ac}/R_{dc}$, for various values of gap pitch, p, and spacing between gap and conductor, s, all for a small gap length, $g = 0.1$. To explain the results qualitatively, we first consider variations in the pitch. As the gap pitch gets larger, F_r increases significantly. This is due to the tendency for current to crowd near the gaps, as shown in Fig. 5. As the gap pitch gets smaller, the region of current crowding becomes a larger fraction of the overall width. When adjacent regions overlap (p equal to one to two skin depths), the current distribution becomes approximately uniform, as shown in Fig. 6. The ac resistance factor approaches a minimum, almost equal to the ac resistance factor with a distributed gap.

Spacing the gaps away from the conductor can also be beneficial for decreased ac losses. In this sense, intuition regarding gap fringing fields is correct. The distance required for any given ac resistance is affected by gap pitch, p, as can be seen in Fig. 4. One may think of this as the myopia of the eddy current losses. If the gaps are far enough away, they "blur out" and "look" like a single distributed gap.

In the above discussions, the gap length g is fixed. To illustrate the effect of gap length on ac losses, we examine the effect of varying gap length on two designs, each with different fixed values of gap pitch and spacing, p and s. The first design represents the case where the original value of F_r is relatively low, while the second one represents the case of a higher original F_r value. The simulation results for the effect of gap length on these two designs are shown in Fig. 7. To explain these results, we return to the idea of current crowding into the region near the gaps. As the gap gets bigger than one skin depth, the width of the gap becomes the dominant factor determining the width of the region of current crowding. Thus a wider gap can spread the current out further and decrease losses, as can be seen by comparing Fig. 8 to Fig. 5. This tendency for wide gaps to reduce current crowding explains the trend in Fig. 7. However, once the gap is small compared to a skin depth, the width of the current crowding region is determined by the skin depth, as illustrated in Fig. 5. Further reductions in gap length have little effect; the current crowding region is about two-skin-depths wide whether the gap length is 0.1 skin depth or 0.01 skin depth. Thus, for gaps small compared to skin depth, ac resistance is independent of gap length, as can be seen in the flat regions in the left portion of Fig. 7.

[2]One could use the lateral symmetry of the structure in Fig. 3 to further shorten simulation time, but this was not convenient with the software tool we used.

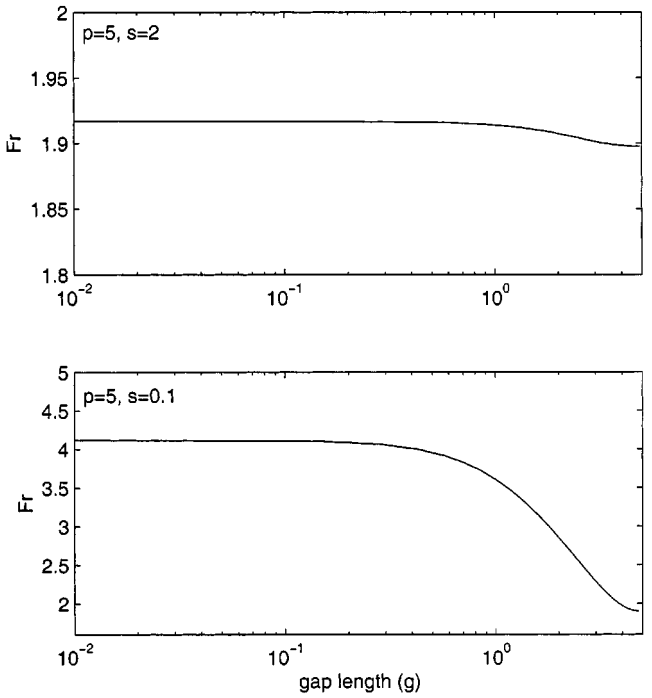

Fig. 7. AC resistance factor, F_r as a function of gap length, g, normalized to one skin depth, for two geometric configurations defined by the normalized values of p and s indicated. (The geometric parameters are defined in Fig. 3.)

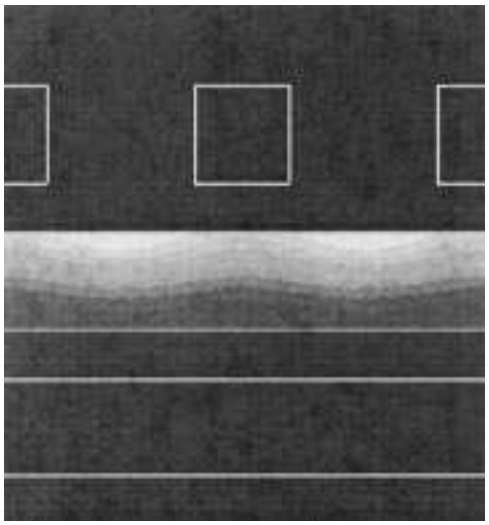

Fig. 8. Current distribution in a cross section of a quasidistributed gap inductor. As in Fig. 5, but with a larger gap length $g = 3$ skin depths.

Although wide gaps can reduce ac losses, this is not useful in most practical situations. For the example shown in Fig. 7(a), changing the gap length does not improve F_r significantly. For the example shown in Fig. 7(b), in order to significantly reduce losses and achieve F_r of about 2.5, the gap length has to be about 50% of the pitch length. This results in an effective permeability of the quasidistributed gap of about 2, too low for most inductor designs. In general, the inductance requirement will constrain the total gap length, g_t, to be a fixed, small fraction of the conductor width w. If n gaps are distributed within a width w, $g = g_t/n$ and $p = w/n$. To get ac losses near those of a true distributed-gap inductor, one might think that the number of gaps, n, should be small in order to make the gap length larger. However, if n is reduced, the gap pitch will also become larger. As shown in Fig. 4, making the gap pitch larger will increase F_r dramatically. Thus, although large gaps can reduce losses, this effect is not of practical importance and the region of interest is that of smaller gap lengths.

In the region of small gaps, Fig. 7 shows that gap length has almost no effect on ac resistance. For example, in Fig. 7(b), a factor of 30 change in g (from 0.01δ to 0.3δ, where δ is the skin depth in the conductor) results in only about a 1.5% reduction in F_r . Note that this includes a range of ratios of spacing to gap length from $s/g = 10$ to $s/g = 0.33$, confirming that a rule of thumb based on making the spacing large compared to the gap length would not be useful.

Most of our simulations use a small gap, $g = \delta/10$, and the results in Fig. 4 are applicable, with less than 1.5% error, to any design with a gap that is small compared to a skin depth ($g < \delta/3$), or small compared to spacing ($g \ll s$). With small gaps, and fixed conductor thickness, F_r may be described as a function of just two variables, the spacing from the gap to the conductor s and the gap pitch p. It is the size of dimensions relative to skin depth that really matters; thus, the data in Fig. 4, where the dimensions are normalized to one skin depth, can be used to determine the ac resistance for any small-gap design. (They directly apply only if the thickness of the conductor is equal to two skin depths. Scaling for other thickness of conductor will be discussed in Section II-F.)

Both in Figs. 4 and 7, the minimum ac resistance factor is about $F_r = 1.9$. A one-dimensional solution of Maxwell's equations yields the following expression for ac resistance factor with a uniformly distributed gap [28]:

$$F_r = \frac{2t_{Cu}\sinh(2t_{Cu}) + \sin(2t_{Cu})}{\cosh(2t_{Cu}) - \cos(2t_{Cu})} \tag{1}$$

where t_{Cu} is the thickness of the conductor normalized to skin depth. For $t_{Cu} = 2$, $F_r = 1.898$, very close to the minimum ac resistance factor of the simulation results.

B. Closed-Form Approximation

In order to facilitate design without the need to use tables or plots of data, an empirical expression to describe F_r as a function of conductor–gap spacing s and gap pitch p is needed. Examining the data in Fig. 4 more closely, we see that F_r as a function of p, for any given s, tends to be asymptotic to two line segments, one for small values of p and one for large values of p, with a smooth transition between the two line segments. A flexible functional form for fitting this type of data is

$$f(x) = \frac{k_1 - k_2}{(b^{-n} + x^{-n})^{1/n}} + k_2 x + C \tag{2}$$

where

- C y-intercept;
- k_1 initial slope (of the first line segment);
- k_2 final slope;
- b breakpoint between the two slopes;
- n exponent determining the abruptness (large n) or smoothness (small n) of the transitions between slopes [29].

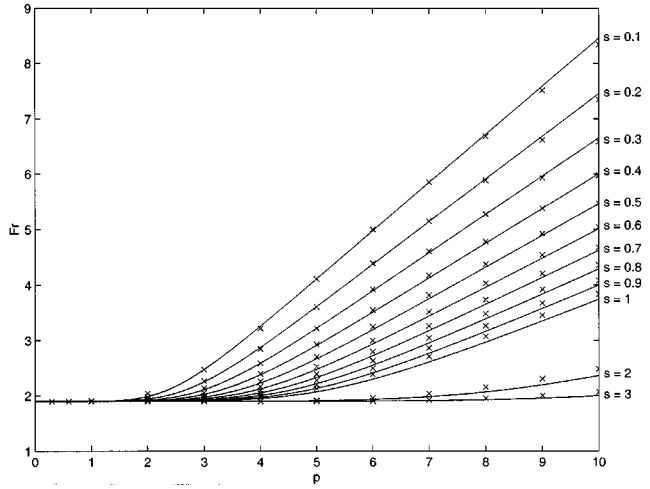

Fig. 9. Comparison between values of F_r computed by using the approximation expression (3) and values obtained from finite-element simulations, as a function of normalized pitch p, for normalized spacing s as indicated. The solid lines show computed values; the $\times$'s mark simulation data.

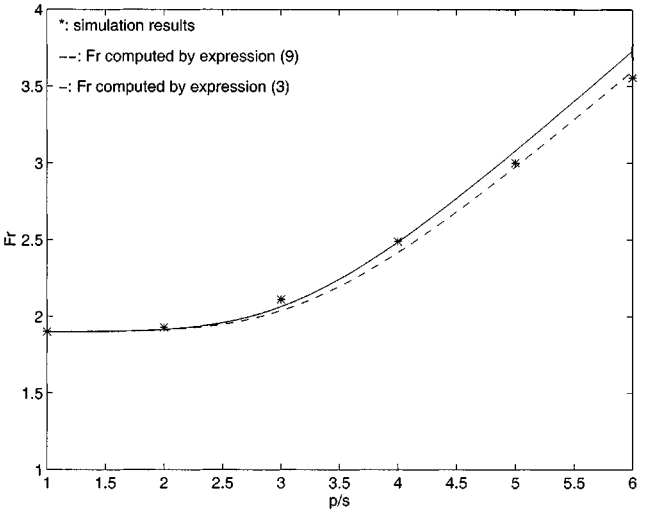

Fig. 10. F_r as a function of the ratio p/s with $s = 20$. The results are approximately the same for any large value of s.

We found that (2) worked well to fit each curve in Fig. 9, using $C = 1.9$, $k_1 = 0$, $n = 5.4$, and values of b and k_2 that vary with s. With $k_1 = 0$ there is only one nonzero $k = k_2$ and so we drop the subscript for simplicity. Similar curve fitting was also applied to finding b and k as functions of s, for which simpler forms were found to be adequate.

The final result of a numerical least-square fit to the data in Fig. 4 for $p = 0.3$ to 10, $s = 0$ to 6, and $g = 0.1$ is the following expression to approximate $F_r(s,p)$ for any design with a gap that is small compared to a skin depth $(g < \delta/3)$, or small compared to spacing $(g \ll s)$, with copper thickness $t_{Cu} = 2$:

$$F_r(s,p) = \frac{-k}{(b^{-n} + p^{-n})^{1/n}} + k \cdot p + 1.9 \tag{3}$$

where

$$n = 5.4, \tag{4}$$

$$k = \frac{0.95}{0.95 + 1.4 \cdot s}, \tag{5}$$

$$b = 3.33 \cdot s + 2.14. \tag{6}$$

The F_r values computed by the above expressions are compared to simulation results in Fig. 9. It can be seen that this expression approximates the simulation results very well, with relative error less than 4.5%, and absolute error in F_r less than 0.08. This expression also remains accurate for configurations with large s and p, as shown in Fig. 10.

For large s, (5) and (6) become

$$k \cong \frac{0.68}{s} \tag{7}$$

$$b \cong 3.33 \cdot s. \tag{8}$$

Using (7) and (8), we can rewrite (3) as

$$F_r = \frac{-0.68}{\left(3.33^{-n} + \left(\frac{p}{s}\right)^{-n}\right)^{1/n}} + 0.68 \cdot \left(\frac{p}{s}\right) + 1.9 \tag{9}$$

showing that F_r depends only on the ratio p/s for large s (i.e., spacing large compared to a skin depth). This approximation is based simply on taking the limit of (3)–(6) for large s, and is not based on any new approximations to experimental simulation data. As shown in the Appendix, the fractional error in the approximation of (3) by (9) is approximately bounded by $0.68/s$. This error is in addition to the error already present in (3), which may be as high as 4.5%. The results of (9) are compared to (3) and to simulation data in Fig. 10, for $s = 20$. In addition to confirming that (9) approximates (3), Fig. 10 also demonstrates the fact that (3)–(6), which were developed based on data with $s \leq 6$, accurately model F_r even for larger conductor–gap spacing, such as, in this case, $s = 20$.

Although (9) loses some accuracy compared to (3) (about 3.4% in this case of $s = 20$), it is often helpful for design purposes because it more directly shows the relationship between ac resistance and the primary variable responsible for controlling it, namely the ratio p/s. For example, one can see from Fig. 10 that a simple design approach is to always choose $p/s \leq 4$ in order to obtain low ac resistance, approaching the minimum attainable. Thus, (9) can be used to aid understanding in the design process, but for the best accuracy in estimating losses, (3) is almost always preferred.

The errors in (9) with respect to (3) lead only to overestimates of loss, as would be desired in a conservative design approximation. However, the error in (3) may be in either direction, such that (9) may slightly underestimate loss in some cases, as can be seen in the third data point in Fig. 10, in which (9) underestimates loss even though it is above (3), because (3) underestimates loss by about 3% at that point.

C. Full Device Versus Periodic Segments

To check the assumption that a complete device with multiple gaps could be modeled by a single segment of a periodic structure, we simulated two-dimensional cross sections of complete devices, as shown in Fig. 11. The gap pitch was 5, the gap length 0.1, and the spacing was varied from 0.1 to 10, all normalized to a skin depth. Both the core and conductor thickness were two skin depths. Some simulations used a symmetry boundary on one side to represent a device in which the current flows in

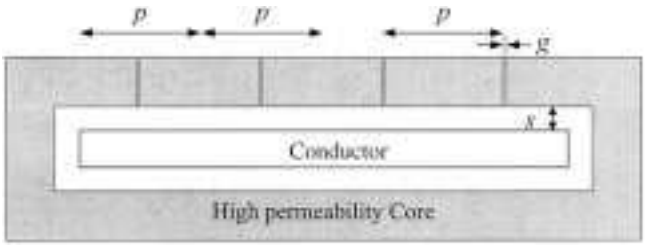

Fig. 11. Full device with four equally distributed gaps.

a planar loop, returning in an adjacent repetition of the structure in Fig. 11. In all these simulations, the ac resistance factor was within 2% of the value obtained from the simulation of a single segment. We conclude that in typical practical designs, the losses are accurately modeled by a single segment.

D. Finite Permeability of Core Material

Throughout the simulations described above, the permeability of the core material was almost infinite, which implies that the reluctance of the core is zero and flux is only determined by the reluctance of the gaps. In a real design, if we consider the effect of the finite reluctance of the core, the fraction of the MMF drop across the core will be higher, while the MMF drop across the gaps will be lower. The MMF drop across the core is similar to the MMF drop in a true distributed gap, and thus, the ac resistance is reduced. In order to illustrate this quantitatively, simulations using finite-permeability core material were performed. For a configuration of $p = 5$ and $s = 1$

$$F_{\mathrm{r}}|_{\mu_{\mathrm{r}}=\infty} \cong 2.13,$$
$$F_{\mathrm{r}}|_{\mu_{\mathrm{r}}=1000} \cong 1.85$$

where μ_{r} is the relative permeability of core material. These results confirm the previous discussion. Note that the ac resistance factor with $\mu_{\mathrm{r}} = 1000$ is less than 1.9, the minimum with a distributed gap as shown in Fig. 1. This is because with low permeability material underneath the conductor, we start to use the bottom surface as well as the top surface to conduct ac current.

E. Thickness of the Core

The simulations that were used to develop the closed-form approximation (3)–(6) all used the same core thickness, equal to two skin depths, and so to use the results more generally, we must consider the effect of different core thicknesses. Fig. 12 shows the ac resistance factor of a design with $p = 6$ and $s = 1$ as a function of core thickness ranging over three orders of magnitude. There is very little variation in ac resistance, which confirms that (3) is valid for any core thickness. With a normalized gap length $g = 0.1$, the variation is well under 0.1%, for core thickness ranging from one tenth to one hundred times the gap length. As the gap length increases, the effect increases, but remains very small: 0.5% at $g = 1$ and 2% at an impractical $g = 3$, half the gap pitch, where the effective relative permeability of the quasidistributed gap is reduced to two.

One can quickly conclude that core thickness is not an important factor, but it is instructive to consider the physical reasons behind this result, which might seem counterintuitive to those

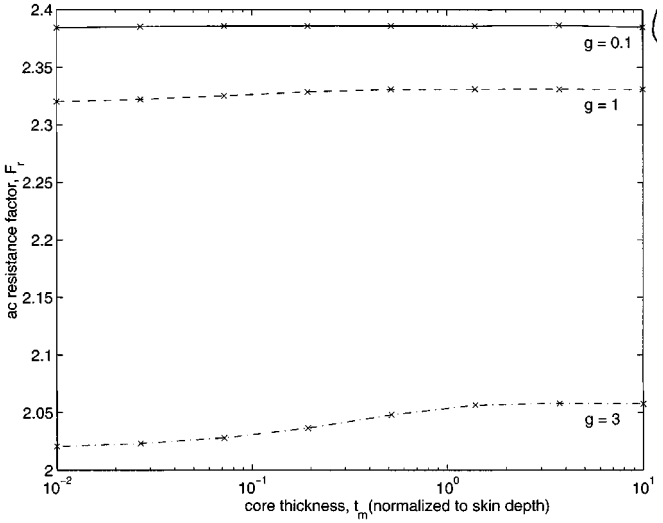

Fig. 12. Effect of core thickness on ac resistance factor, from simulation data for normalized parameters $s = 1$, $p = 6$. The slight effect, approaching significance only for very long gaps outside the scope of (3) confirms that (3) is valid for any core thickness.

used to considering the effect of fringing fields on gap reluctance, which are greatest when $t_{rmm} \ll g$ and become negligible when $t_{rmm} \gg g$. The following explanation may also be helpful in elucidating the reason that varying gap length has little effect on ac resistance until the gap length becomes large compared to the pitch, or, for small spacings, becomes large compared to skin depth.

For considering ac resistance effects, we are interested in the effect fringing fields have on the conductor in the winding window, not on the relative magnitude of this flux versus the flux in the gap, which would be the important factor for considering fringing effects on inductance. The quasidistributed gap serves to define boundary conditions for the field solution in the region of the winding window. Specifically, the MMF generated by the winding will be dropped equally across each gap, and each core segment between gaps will be at a constant MMF potential. With small gaps, the MMF at the top of the winding window is a series of abrupt steps. For a given winding current, the magnitude of these steps is not affected by the gap length, which only affects the steepness of the transition between steps, as illustrated in Fig. 13. For small gaps, the boundary conditions are similar for a wide range of gap sizes, which explains the left portion of the curves in Fig. 7, where gap length has almost no effect on ac resistance. As the gap becomes longer, the transition between steps becomes a significant portion of the boundary condition, and the shape of the transition in the MMF step can have an effect on the ac resistance. When the core thickness is large compared to the gap, as in Fig. 13(b), the transition is approximately linear. However, when the core is thin compared to the gap, the flux crowding at the ends of the gap results in a steeper MMF drop is these areas [Fig. 13(c)]. Thus, the effect of the gap is concentrated toward its outer edges, which helps to slightly spread the region of current crowding and very slightly lower the ac resistance, as can be seen in the left portion of the $g = 3$ curve in Fig. 12. This case is discussed only for the insight it lends into the behavior of ac resistance with quasidistributed gaps; in practice, the effect of core thickness is negligible.

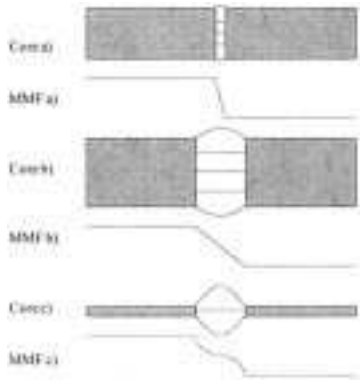

Fig. 13. Three core structures with flux lines sketched and the corresponding MMF diagrams. Core thickness has very little effect on the MMF boundary conditions of the winding window. Only when the gap length is long does the effect have any significance, but even then the effect is slight. These sketches are not intended to be quantitatively accurate.

F. Thickness of the Conductor

In the discussion above the thickness of the conductor is fixed to be two times the skin depth. Although increasing the thickness of the conductor will lower the dc resistance, it will not improve the ac resistance significantly. Given a thickness other than two skin depths, we can estimate $F_{\rm r}$ based on constant ac resistance as

$$F_{\rm r}(t_{rmm}=x) \cong F_{\rm r}(t_{rmm}=2)\frac{x}{2}. \tag{10}$$

This is valid when the conductor thickness is greater than one skin depth, as illustrated in Fig. 14. Typical errors in this approximation are 2 to 5%, but can exceed 10% for $t_{\rm Cu}$ near one skin depth.

III. Design Rules

Based on the above analyses, we can glean the following design rules. Low ac losses (ac resistance factor less than 2.5, approaching that of a distributed-gap inductor), can be obtained if either of the following conditions are met.

1) The ratio of gap pitch to conductor–gap spacing (p/s) is less than four.
2) The gap pitch p is less than 2.5 times skin depth.

In practice, one wishes to avoid small gap pitch because it is expensive, and one wishes to avoid large spacing, because of packaging constraints, so it is not immediately clear which of these criteria to follow. However, skin depth is very small for the frequencies of interest, 70 to 220 μm for the 100 kHz to 1 MHz frequency range, and a gap pitch of 0.5 mm or less would be required by the second design rule. Meeting the first criterion is often much easier. For example, with a 1-mm conductor–gap spacing, a 4-mm gap pitch is required. This is much more practical, requiring only an eighth as many gaps.

If the gap length g is sufficiently large, it can also reduce the ac resistance. However g must be a substantial fraction of the gap pitch p to have tangible effect on ac resistance. This is unlikely to be practical in most designs.

It is interesting to note that these design rules are consistent with the results in both [6] and [14]. In each of these papers, one particular design was optimized by repeated simulation, but no attempt was made to generalize the results, as has been done here.

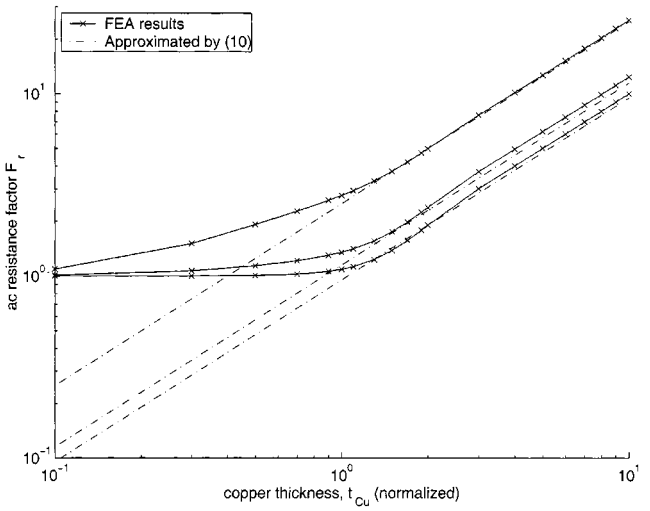

Fig. 14. Effect of conductor thickness on ac resistance factor. Points marked with $\times$ and joined with solid lines are FEA simulation results. The simple approximation (10), shown with dotted lines, provides a good fit for conductor thickness greater than one skin depth. The normalized geometrical parameters for the curves are, from top to bottom, for $s = 0.1$, $s = 1$, and $s = 3$; all for $p = 6$ and $g = 0.1$.

One of the advantages of the closed-form approximation developed here is that it can be used to quickly and easily evaluate the sensitivity of a design to tolerances in the geometry. This is in contrast to a design produced by direct application of trial-and-error finite-element analysis, which would require additional simulations to evaluate its sensitivity.

IV. Design Example

Consider the design of an inductor for a high-current, low-voltage voltage regulator module (VRM) for microprocessor power delivery. A buck converter with high ripple current in the inductor, in order to allow fast response time, is emerging as the standard solution for this application [30], [31], often with multiple interleaved phases. Low ac resistance is important because of the high ripple current in the inductor. We consider a design for 7 A dc current for a single phase of such a converter switching at 1 MHz, with a 5 V input and a 1 V output. With 100 nH inductance, the peak-to-peak ripple current is 8 A, such that the current ranges between a minimum of 3 A and a maximum 11 A over a switching cycle. In this design example we illustrate two ways to apply the model developed in this paper. First, we use the new qualitative understanding and design rules to quickly produce a plausible winding design. Next, we use the closed-form ac resistance approximation to estimate the ac resistance of the design. Another way that we expect our results to be useful is in formal optimization in which parameters are adjusted to optimize specific objectives such cost, loss and size, but such optimization is not illustrated in this example.

At high current and low voltage, consideration of the tradeoff between core and winding loss leads to a single-turn design. Also because of the low-impedance application, termination resistance can introduce significant loss, and a winding integrated into a PC board is desirable. In order to minimize the cost, the

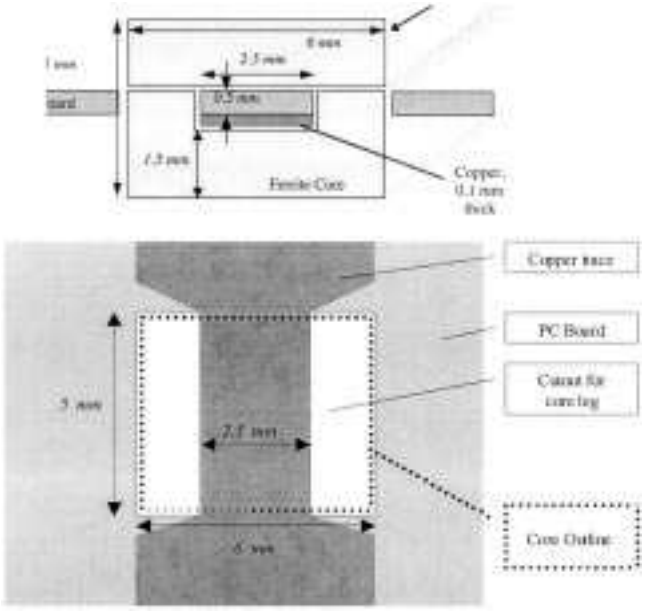

Fig. 15. Example of a design for which the techniques described here allow accurate predictions, even though the geometry does not exactly match that in Fig. 2. The top sketch is a cross-section; the bottom is a plan view of the PC board in the immediate vicinity of the inductor.

number of core segments used to construct the quasidistributed gap should be minimized. According to the design rule $p/s \leq 4$, a larger spacing allows maximizing pitch and minimizing the number of segments. However, minimizing the height of the component is desirable for high-density packaging. Using the 0.5 mm thickness of the PC board substrate for spacing allows up to 2 mm gap pitch; from Fig. 9 we see that using a gap pitch of five times the spacing (2.5 mm) will not severely increase ac resistance. In fact, 2.5 mm is in fact wide enough to serve as the whole width of the inductor, and thus an inductor could be constructed as shown in Fig. 15. The inductor uses a single-turn winding fabricated as a trace on a PC board, with a ferrite core assembled around the board. The two pieces of the core are assembled with a small gap (0.06 mm) to get the required inductance of 100 nH.

The gaps in Fig. 15 are oriented perpendicular to the gaps in a standard quasidistributed gap structure. However, this has little effect on the field within the winding window, because the boundary conditions around the border of the window are only affected by where the gaps appear in that boundary. This is similar to the reason that core thickness is unimportant, as discussed in Section II-E. As confirmed in detail below, the only significant difficulty introduced by the new gapping structure is the indeterminacy in the definition of s; whether to include g in the value of s.

The resistance in the new design may be quantitatively estimated, starting with a simple calculation of the dc resistance as 0.345 mΩ, based on a copper conductivity of 5.8×10^7 S. For a quick estimate of ac resistance, we can use (9) with a value of $p/s = 5$ to obtain $F_r = 3.08$ for a conductor two-skin-depths thick. However, since the conductor is 1.51 skin depths thick, we must modify this result with (10) to obtain $F_r = 2.33$, and thus an ac resistance of 0.80 mΩ. For a more careful calculation, we can use (3). It is not immediately clear whether to include the length of the gap in s for this geometry, so calculations are performed both ways. Using just the distance from the conductor to the bottom of the gap, 0.5 mm, for s, we find, from (3), $F_r = 2.83$, which, modified by (10), gives an ac resistance of 0.738 mΩ. The same calculation including the gap in s yields an ac resistance of 0.667 mΩ. Comparing these to a finite-element simulation, which gives an ac resistance of 0.655 mΩ, we see that the errors are 23% for the quick estimate, 13% using (3) without g included in s and 1.8% with g included. We see, in hindsight, that including g in s is best; without this knowledge, one might guess to include $g/2$ in s, which would have resulted in 7% error.

TABLE I
ERROR SOURCES IN APPLICATION TO EXAMPLE DESIGN

Error Source	s includes g	s does not include g
Fit of (3) to simulation of configuration in Fig. 3 for these parameters	2.0%	2.0%
Effect of horizontal gap orientation	0.3%	0.3%
Accuracy of thickness scaling (10)	-2.1%	-2.1%
Effect of including or omitting g in s	2.2%	-8.5%
Effect of finite permeability (2000)	-3.2%	-3.2%

The above are the cumulative results of the errors from many sources. To determine how different error sources contributed to these total errors, a set of further simulations was conducted, varying one parameter at a time between the ideal structure in Fig. 3 and the design in Fig. 14, with results summarized in Table I. The fundamental accuracy of the closed-form approximation (3) for these values of p and s is 2%. The application of the same analysis to a configuration with gaps at the corners of the window, oriented outward instead of upward, introduces only 0.3% error, as determined by a simulation using a much smaller gap. However, the uncertainty of the proper value to use for s introduces up to 8.5% error without g included in s, but it is more accurate to include g in s, in which case the error due to this effect is only 2.2%.

This example illustrates the applicability of this method to a design that would not ordinarily be considered a quasidistributed gap. The simple rule to choose $p/s \leq 4$ proved useful as a quick guide to a design that would have low ac resistance. The simplified formula based on p/s (9) provided a quick estimate of ac resistance with about 23% error in this case. More careful analysis using (3) resulted in error of 2% to 13%, with most of the error being due to the uncertainty in defining the parameter s for this geometry.

V. CONCLUSION

Simulation of a single segment of a periodic quasidistributed gap inductor is adequate to predict the ac resistance. A set of such simulations produces data that can be used for a wide range of designs. Approximate analytic formulae that describe these

data accurately have been developed. This has led to a simple set of design rules that can be used to ensure a design that will have low ac resistance. The most widely useful design rule is to keep the spacing between the winding and the gap larger than one-quarter the pitch (spacing between gaps). The gap length is ordinarily not an important factor, although unusually large gaps can slightly decrease ac resistance. A design example of a PCB-based inductor for a high-current, low-voltage, fast-response VRM demonstrates the utility of the method.

The principal limitation of the results we have presented is that they apply only to single winding layers with copper thickness greater than one skin depth. We have shown that for such windings, $p/s \leq 4$ leads to ac resistance close to that of a distributed-gap inductor. It is likely that the same general guideline applies to multilayer windings with thin layers. This is consistent with the results in [6], [14]. However, additional work would be needed to develop quantitative predictions for multilayer windings and for the thin layers that are advantageous in multilayer windings. Another limitation of the results presented here is that they address only planar windings, and do not apply to round-wire or litz-wire windings. This limitation is not, however, expected to be of much practical importance, as it has been found that a less expensive strategy—optimizing the placement of wire turns within the winding window—can not only equal but surpass the performance of an ideal distributed gap design [32], [33].

APPENDIX
ERROR ESTIMATE FOR SIMPLIFIED AC RESISTANCE EXPRESSION

As illustrated in Fig. 10, the simplified ac-resistance-factor expression (9) tends to slightly overestimate the ac-resistance factor given by (3). The degree of overestimation is worst, for any given value of s, toward high p/s, where (3) is asymptotic to

$$F_{\mathrm{r}} = \frac{0.68\frac{p}{s}}{1+\frac{0.68}{s}} - \frac{2.26}{1+\frac{0.68}{s}} + 1.9 \tag{11}$$

and (9) is asymptotic to

$$F_{\mathrm{r}} = 0.68\frac{p}{s} - 0.36. \tag{12}$$

Comparing (11) and (12) leads to the conclusion that the fractional error in using (9) to approximate (3) is approximately bounded by $0.68/s$. For example, in Fig. 10, where $s = 20$, this gives a 3.4% error estimate, consistent with Fig. 10, and consistent with the idea that (9) is useful in guiding design, but that (3) is preferred for higher accuracy. It is important to note that (3) is an approximate expression to begin with, and $0.68/s$ is an estimate only of the error in approximating (3) with (9) not the total error in (9) which also includes the error in (3), which can be as high as 4.5%.

REFERENCES

[1] K. D. T. Ngo and M. H. Kuo, "Effects of air gaps on winding loss in high-frequency planar magnetics," in *Proc. 19th Annu. Power Electron. Spec. Conf.*, Apr. 1988, pp. 1112–1119.

[2] W. M. Chew and P. D. Evans, "High frequency inductor design concepts," in *Proc. 22nd Annu. Power Electron. Spec. Conf.*, June 1991, pp. 673–678.

[3] A. F. Goldberg, J. G. Kassakian, and M. F. Schlect, "Issues related to 1–10 MHz transformer design," *IEEE Trans. Power Electron.*, vol. 4, pp. 113–123, Jan. 1989.

[4] C. R. Sullivan and S. R. Sanders, "Design of microfabricated transformers and inductors for high-frequency power conversions," *IEEE Trans. Power Electron.*, vol. 11, pp. 228–238, Mar. 1996.

[5] L. Daniel, C. R. Sullivan, and S. R. Sanders, "Design of microfabricated inductors," *IEEE Trans. Power Electron.*, vol. 14, pp. 709–723, July 1999.

[6] U. Kirchenberger, M. Marx, and D. Schroder, "A contribution to the design optimization of resonant inductors in high power resonant converters," in *Proc. IEEE Ind. Applicat. Soc. Annu. Meeting*, vol. 1, Oct. 1992, pp. 994–1001.

[7] M. Meinhardt, M. Duffy, T. O'Donnell, S. O'Reilly, J. Flannery, and C. O. Mathuna, "New method for integration of resonant inductor and transformer—design, realization, measurements," in *Proc. Appl. Power Electron. Conf. (APEC'99)*, vol. 2, 1999, pp. 1168–1174.

[8] W. A. Roshen, R. L. Steigerwald, R. J. Charles, W. G. Earls, G. S. Claydon, and C. F. Saj, "High-efficiency, high-density MHz magnetic components for low profile converters," *IEEE Trans. Ind. Applicat.*, vol. 31, pp. 869–878, July/Aug. 1995.

[9] N. H. Kutkut, D. W. Novotny, D. M. Divan, and E. Yeow, "Analysis of winding losses in high frequency foil wound inductors," in *Proc. IEEE Ind. Applicat. Conf. 30th IAS Annu. Meeting*, Oct. 1985, pp. 859–867.

[10] N. H. Kutkut and D. M. Divan, "Optimal air gap design in high frequency foil windings," in *Proc. IEEE Appl. Power Electron. Conf.*, Atlanta, GA, Feb. 1997.

[11] ——, "Optimal air-gap design in high-frequency foil windings," *IEEE Trans. Power Electron.*, vol. 13, pp. 942–949, Sept. 1998.

[12] N. H. Kutkut, "A simple technique to evaluate winding losses including two-dimensional edge effects," *IEEE Trans. Power Electron.*, vol. 13, pp. 950–958, Sept. 1998.

[13] M. A. Preston, R. W. DeDoncker, R. C. Oney, C. M. Stephens, and M. Hernes, "High-current high-frequency inductors for resonant converters," in *Proc. Euro. Conf. Power Electron. Applicat.*, Florence, Italy, Sept. 1991, pp. 242–246.

[14] A. Nysveen and M. Hernes, "Minimum Loss Design of a 100 kHz Inductor with Foil Windings," in *Proc. Euro. Conf. Power Electron. Applicat.*, London, U.K., Sept. 1993, pp. 106–111.

[15] P. Wallmeier, N. Frohleke, and H. Grotstollen, "Improved analytical modeling of conductive losses in gapped high-frequency inductors," in *Proc. IEEE Ind. Applicat. Conf.*, St. Louis, MO, Oct. 1998, pp. 913–920.

[16] J. Hu and C. R. Sullivan, "The quasi-distributed gap technique for planar inductors: design guidelines," in *Proc. IEEE Ind. Applicat. Conf.*, vol. 2, 1997, pp. 1147–1152.

[17] F. Robert, P. Mathys, and J.-P. Schauwers, "A closed-form formula for 2-D ohmic losses calculation in SMPS transformer foils," in *Proc. Appl. Power Electron. Conf. (APEC'99)*, 1999, p. 199.

[18] J. Reinert, A. Brockmeyer, and R. W. De Doncker, "Calculation of losses in ferro- and ferrimagnetic materials based on the modified Steinmetz equation," in *Proc. 34th Annu. Meeting IEEE Ind. Applicat. Soc.*, vol. 3, 1999, pp. 2087–2092.

[19] W. K. Mo, D. K. W. Cheng, and Y. S. Lee, "Simple approximations of the dc flux influence on the core loss power electronic ferrites and their use in design of magnetic components," *IEEE Trans. Ind. Electron.*, vol. 44, pp. 788–799, Dec. 1997.

[20] A. Brockmeyer and J. Paulus-Neues, "Frequency dependence of the ferrite-loss increase caused by premagnetization," in *Proc. 12th Annu. Appl. Power Electron. Conf. Expo.*, 1997, p. 375-380.

[21] W. G. Hurley, E. Gath, and J. G. Breslin, "Optimizing the ac resistance of multilayer transformer windings with arbitrary current waveforms," *IEEE Trans. Power Electron.*, vol. 15, pp. 369–376, Mar. 2000.

[22] A. F. Goldberg, J. G. Kassakian, and M. F. Schlecht, "Finite-element analysis of copper loss in 1–10 MHz transformers," *IEEE Trans. Power Electron.*, vol. 4, pp. 157–167, Mar. 1989.

[23] L. Ye, G. R. Skutt, R. Wolf, and F. C. Lee, "Improved winding design for planar inductors," in *Proc. 28th Annu. IEEE Power Electron. Spec. Conf. (PESC'97)*, vol. 2, 1997, pp. 1561–1567.

[24] G. Skutt, F. C. Lee, R. Ridley, and D. Nicol, "Leakage inductance and termination effects in a high-power planar magnetic structure," in *Proc. IEEE Appl. Power Electron. Conf. Expo. (APEC'94)*, vol. 1, 1994, pp. 295–301.

[25] G. R. Skutt and P. S. Venkatraman, "Analysis and measurement of high-frequency effects in high-current transformers," in *Proc. 5th Annu. Appl. Power Electron. Conf. Expo. (APEC'90)*, 1990, pp. 354–364.
[26] P. Alou, J. A. Cobos, R. Prieto, J. Uceda, and M. Roascon, "Influence of windings coupling in low-voltage dc/dc converters with single winding self-driven synchronous rectification," in *Proc. Appl. Power Electron. Conf. (APEC'00)*, vol. 2, 2000, pp. 1000–1005.
[27] R. Prieto, J. A. Cobos, O. Garcia, P. Alou, and J. Uceda, "Model of integrated magnetics by means of "double 2D" finite element analysis techniques," in *Proc. 30th Annu. IEEE Power Electron. Spec. Conf.*, vol. 1, 1999, pp. 598–603.
[28] R. L. Stoll, *The Analysis of Eddy Current*. Oxford, U.K.: Clarendon, 1974.
[29] C. R. Sullivan and S. R. Sanders, "Models for induction machines with magnetic saturation of the main flux path," *IEEE Trans. Ind. Applicat.*, vol. 31, pp. 907–917, July–Aug. 1995.
[30] B. Arbetter and D. Maksimovic, "DC–DC converter with fast transient response and high efficiency for low-voltage microprocessor loads," in *Proc. 13th Annu. Appl. Power Electron. Conf. Expo. (APEC'98)*, 1998, p. 156.
[31] X. Zhou, X. Peng, and F. C. Lee, "A high power density, high efficiency and fast transient voltage regulator module with a novel current sensing and current sharing technique," in *Proc. Appl. Power Electron. Conf. (APEC'99)*, 1999, p. 289.
[32] J. Hu and C. R. Sullivan, "Optimization of shapes for round-wire high-frequency gapped-inductor windings," in *Proc. IEEE Ind. Applicat. Soc. Annu. Meeting*, 1998, pp. 900–906.
[33] ——, "Analytical method for generalization of numerically optimized inductor winding shapes," in *Proc. 30th Annu. IEEE Power Electron. Spec. Conf.*, 1999.

Jiankun Hu received the B.E. degree in mechanical and electrical engineering from the University of Science and Technology of China, Hefei, and the M.S. degree in electrical engineering from Dartmouth College, Hanover, NH.

He is Member of Technical Service, Agere Systems (formerly Lucent Microelectronics division), Allentown, PA. Previously, he worked as Electrical Design Engineer at GE Fanuc Automation.

Charles R. Sullivan (M'93) was born in Princeton, NJ, in 1964. He received the B.S. degree in electrical engineering (with highest honors) from Princeton University, Princeton, NJ, in 1987 and the Ph.D. degree in electrical engineering from the University of California, Berkeley, in 1996.

Between 1987 and 1990, he worked at Lutron Electronics, Coopersburg, PA, developing high frequency dimming ballasts for compact fluorescent lamps. He is presently Assistant Professor at the Thayer School of Engineering, Dartmouth College, Hanover, NH. He has published technical papers on topics including thin-film magnetics for high frequency power conversion; magnetic component design optimization; dc–dc converter topologies; energy and environmental issues; and modeling, analysis, and control of electric machines.

Dr. Sullivan received the National Science Foundation CAREER Award in 1999 and the IEEE Power Electronics Society Prize Paper Award in 2000.